Preprint Title	Thienothiophene based organic light-emitting diode: synthesis, photophysical properties and application
Authors	Recep Isci and Turan Ozturk
Publication Date	10 Juli 2023
Article Type	Full Research Paper
Supporting Information File 1	BJOC-Supporting Information.docx; 3.3 MB
ORCID® iDs	Recep Isci - https://orcid.org/0000-0003-3086-4478; Turan Ozturk - https://orcid.org/0000-0003-3777-5320

Thienothiophene based organic light-emitting diode: synthesis, photophysical properties and application

Recep Isci[1] and Turan Ozturk[1,2,*]

Address: [1]Department of Chemistry, Istanbul Technical University, 34469, Maslak, Istanbul, Turkey and [2] TUBITAK UME, Chemistry Group Laboratories, 41470, Gebze, Kocaeli, Turkey.

*Corresponding: Turan Ozturk (ozturktur@itu.edu.tr)

Abstract

A donor-p-acceptor (D–p–A) type pull–push compound, **DMB-TT-TPA**, of triphenylamine as a donor and dimesitylboron as an acceptor, linked through a thieno[3,2-*b*]thiophene (TT) p-conjugated linker bearing 4-MeOPh group, was designed, synthesized and fabricated as an emitter *via* a solution process for an organic light-emitting diode (OLED) application. **DMB-TT-TPA** exhibited absorption and emission maximums of 411 and 520 nm, respectively, with a mega Stokes shift of 109 nm and fluorescence quantum yields both in solid-state (41%) and in solution (86%). The optical properties were supported by computational chemistry using density functional theory for optimized geometry and absorption. A solution-processed OLED was fabricated using low turn-on voltage, which had performances with maximum power, current and external quantum efficiencies of 6.70% lm.W^{-1}, 10.6 cd.A^{-1} and 4.61%, respectively.

Keywords

thienothiophene; triphenylamine; organoboron; OLED; solution processes

Introduction

In recent years, organic electronic has become very attractive due to its various advantages such as high flexibility, easy designability, low fabrication cost, easy processing and large-scale fabrication [1-4]. Especially in display technology, organic-based materials have been used in many application areas such as OLED, micro-LED, LCD, laser and photodiode by applying thin film method and solution process [5-8]. The performance of organic electronic is based on active layer composition as well as fabrication methods and processing parameters. The organic active layers have been composed of various aromatic p-conjugated small molecules/polymers including thiophene, anthracene, carbazole and triphenylamine [9-13].

Thienothiophenes are two annulated thiophene rings having four isomers, among which the most widely used form is thieno[3,2-*b*]thiophene (TT) [14-19]. They are electron rich, flat and electron delocalized systems. These structural properties make them promising materials to construct conjugated energy-based semiconductors for OLEDs [20-23], perovskite solar cells [24,25], organic field-effect transistors (OFETs) [26-28], capacitors [29,30], hybrid films [31] and photosensitizers [32-34]. Another important p-conjugated unit is triphenylamine (TPA), having 6.80 eV ionization potential, lower than many organic cores, providing a strong electron donating ability for organic electronic applications [12,35]. Dimesitylboron (DMB), with its unoccupied p-orbital, is an electron acceptor organoboron compound used in several donor-acceptor systems to provide the system with pull-push interaction [36,37].

In this work, we have designed and synthesized a D-p-A model pull-push fluorophore, **DMB-TT-TPA**, having TPA and DMB units as donor and acceptor linked through 4-MeOPh substituted TT core as a p-spacer. The photophysical properties of the fluorophore were investigated by spectroscopic methods. Moreover, **DMB-TT-TPA** was fabricated as an emitter for organic light-emitting diode applying a solution process. **DMB-TT-TPA** displayed excellent performances both in device application and as photophysical properties, i.e. maximum solution fluorescence quantum yield of 86% in THF, maximum solid-state fluorescence quantum yield of 41%, maximum current efficiency of 10.6 cd/A and maximum power efficiency of 6.70% lm/W.

Results and Discussion

Design and Synthesis

A donor-p-acceptor (D-p-A) type material, **DMB-TT-TPA**, was synthesized following our method reported previously [20-23,36]. Initially, synthesis of the core unit, thieno[3,2-*b*]thiophen **3**, was conducted starting from 3-bromothiophene **1**, from which monoketone **2**, was constructed in one-pot three step reaction in 83% yield, i.e. (i) lithiation of **1** with *n*-butyllithium at -78 °C, (ii) additions of elemental sulfur and, then, (iii) 2-bromo-1-(4-methoxyphenyl)ethanone. The ring closure reaction in the presence of polyphosphoric acid in refluxing chlorobenzene gave **3** (TT) in 86%, which was brominated with NBS to obtain the brominated TT **4** in 88% yield. TPA-borolane (**6**) was constructed in one-pot two step reaction in 83% yield, i.e. (i) lithiation of **5** with *n*-butyllithium at -78 °C and (ii) addition of 2-isopropoxy-4,4,5,5-tetramethyl-1,3,2-dioxaborolane. The mono-brominated TT (**4**) was subjected to palladium (0) catalyzed Suzuki coupling with TPA-borolane (**6**) to give **7** in 81%, lithiation of which with *t*-BuLi and then addition of dimesitylboron fluoride produced the target D-p-A material, **DMB-TT-TPA**, in 85% yield (Scheme 1).

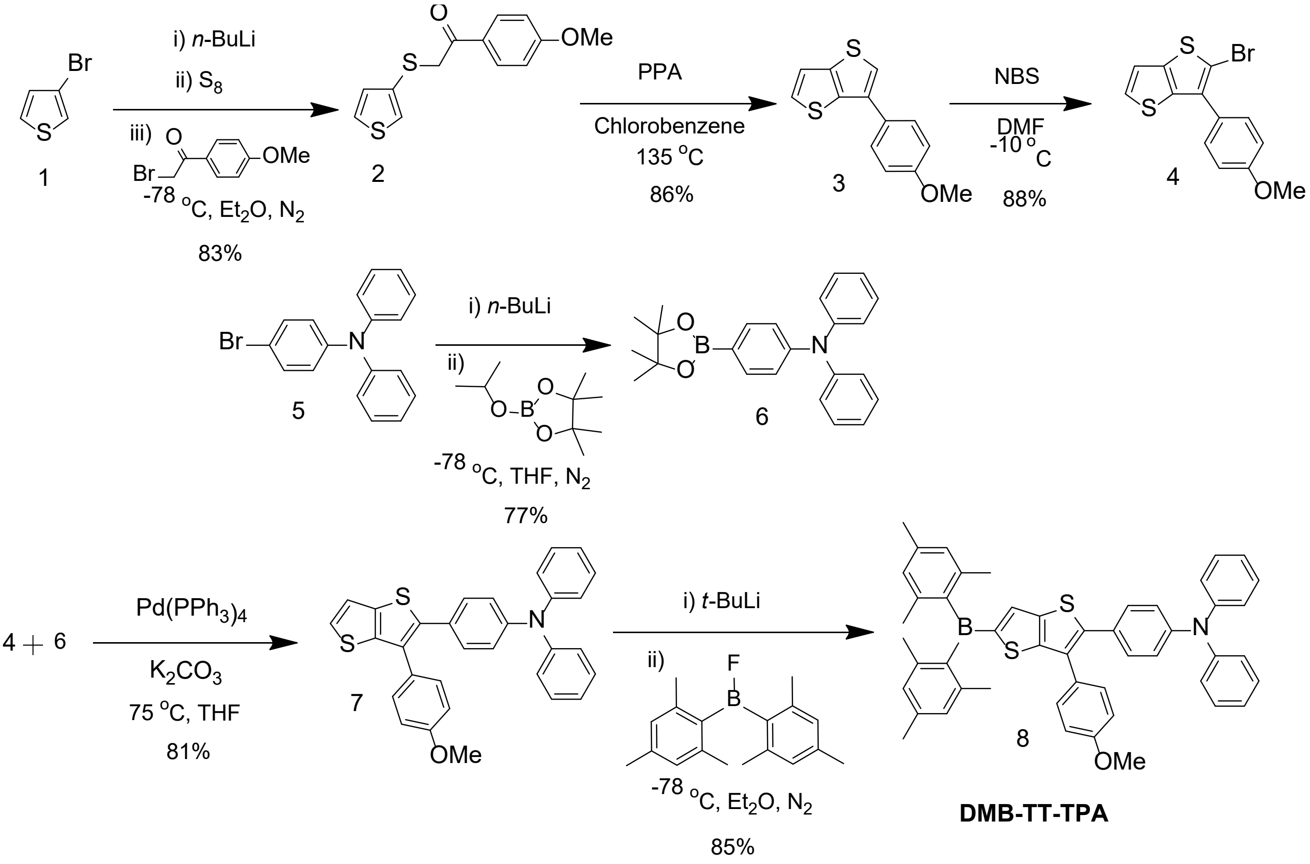

Scheme 1: Synthesis of **DMB-TT-TPA.**

Photophysical Properties

The optical properties (UV-Vis absorption and emission spectra) of **DMB-TT-TPA** were investigated in THF at room temperature (Figure 1 and Table 1). It showed maximum absorption and emission wavelengths of 411 and 520 nm (ex. at λmax), respectively, producing a mega Stokes shift of 109 nm (5100 cm^{-1}), which is due to a fast relaxation from excited state to ground state as a result of strong intramolecular energy-transfer between triphenylamine and boron units through thieno[3,2-*b*]thiophene (TT). The optical band gap (E_{optic}) of **DMB-TT-TPA** was calculated to be 2.52 eV from the onset threshold wavelength of the absorption spectra at 491 nm. It displayed high solid-state and in solution (THF) quantum efficiencies of 41 and 86%, respectively. The remarkable quantum efficiencies indicated that **DMB-TT-TPA** is among the best D-p-A modal fluorophores suitable for an OLED application.

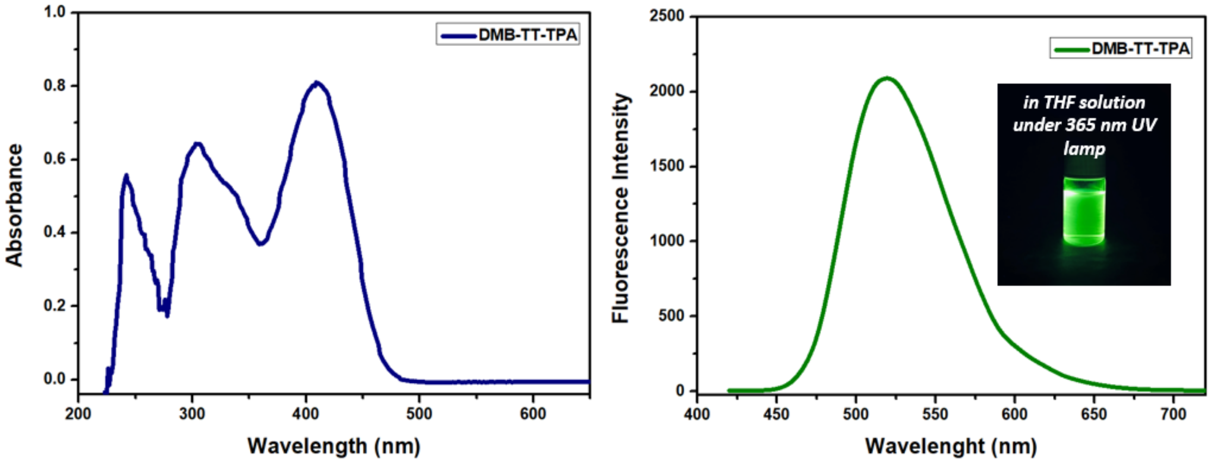

Figure 1: Absorption and emission of **DMB-TT-TPA** in THF. Figure 1 was adapted with permission of Institution of Chemical Engineers (IChemE) and The Royal Society of Chemistry from [38] (“Cationic and radical polymerization using a boron–thienothiophene–triphenylamine based D-π-A type photosensitizer under white LED irradiation”) by A. Suerkan et al., Mol. Syst. Des. Eng., vol. 8, issue 10, © 2023); permission conveyed through Copyright Clearance Center, Inc. This content is not subject to CC BY 4.0.

Table 1: Photophysical data of **DMB-TT-TPA.**

Compound	UV_{max}^{a} (nm)	UV_{onset} (nm)	Fl_{max}^{a} (nm)	Δv^{b} (cm^{-1})	E_{optic}^{c} (eV)	Φ_{solid}^{d} %	Φ_{sol}^{e} %
DMB-TT-TPA	411	491	520	5100	2.52	41	86

[a] Absorption and fluorescence maxima in THF. [b] Stokes shift (cm^{-1}) $\Delta v = 1/\lambda_{max} - 1/\lambda_{em}$. [c] E_{optic} from the onset of absorption spectra. [d] Solid state quantum yield. [e] Solution state quantum yield in THF.

OLED Application

An OLED was fabricated using a standard conventional device architecture of ITO/PEDOT: PSS/TFB/TAPC: TCTA: emitter (**DMB-TT-TPA**) /TPBi /LiF/Ca/Ag, where TFB, TCTA/TAPC and TPBi acted as hole transport, hole transporting host and electron transport materials, respectively (Figure S1). The current efficiency-luminance-voltage (J-LV) graph and power efficiency (PE), external quantum efficiency (EQE) and electroluminescence curves were depicted in Figures 2 and 3, respectively. The OLED of **DMB-TT-TPA** showed a low turn-on voltage (V_{on}) of 2.90 V, max current efficiency (CE_{max}) of 10.6 cd/A, max luminance of 752 cd/m^2, max power efficiency (PE_{max}) of 6.70 lm/W and external quantum efficiency (EQE) of 4.61%, along with a green emitting luminescence at 512 nm. According to the CIE color space chromaticity diagram, the device was located at the coordinates of 0.16 and 0.51. The obtained EL results are in good agreement with the fluorescence characteristic of **DMB-TT-TPA**. In terms of the TT chemistry, the device results reached remarkable values for donor-p-acceptor type solution processable emitters within donor-acceptor family [38-41].

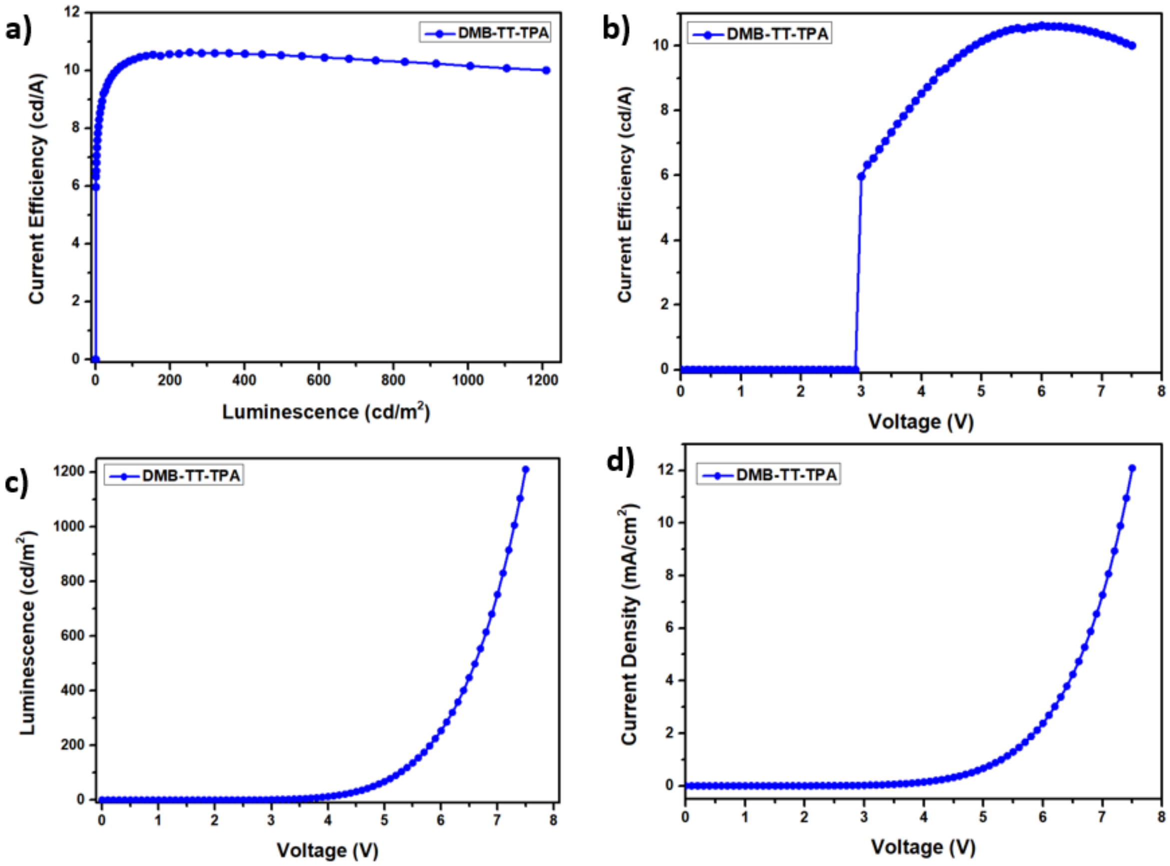

Figure 2: (a) Current Efficiency-Luminance, (b) Current Efficiency-Voltage, (c) Luminance-Voltage and (d) Current Density-Voltage characteristics of the **DMB-TT-TPA**.

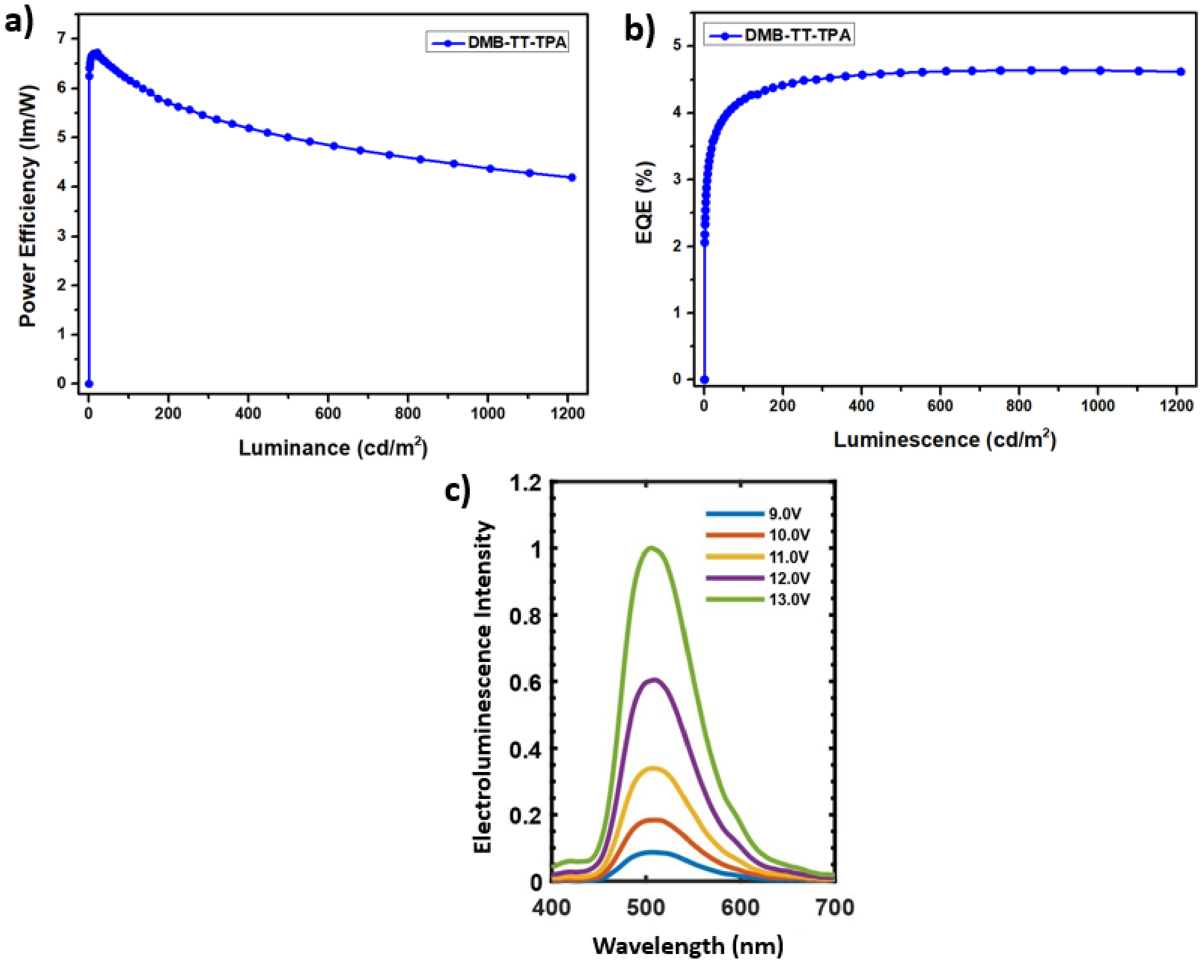

Figure 3: (a) Power Efficiency-Luminance, (b) External Quantum Efficiency-Luminescence, (c) Electroluminescence-Wavelength characteristics of the **DMB-TT-TPA.**

Table 2: Photophysical data of **DMB-TT-TPA.**

Molecule	V_{on} [a] (V)	CE [b] (cd/A)	L [c] (cd/m^2)	I_{EL} [d] (nm)	EQE [e] (%)	PE_{max} [f] (lm/W)	CIE [g] (x, y)
DMB-TT-TPA	2.9	10.6	752	512	4.61	6.70	(0.16, 0.51)

[a]Turn-on voltage, recorded at the luminance of 1 cd.m^2. [b]Maximum current efficiency. [c]Maximum luminance. [e]Maximum electro-luminescence wavelength. [d]Maximum current efficiency. [e]Maximum external quantum efficiency. [f] Maximum power efficiency. [g]Chromaticity coordinates according to the CIE 1931 diagram.

Thermal Properties

The thermal properties of **DMB-TT-TPA** were investigated through thermal gravimetric analysis (TGA) at 750 °C at a heating rate of 10 °C min^{-1} under N_2 atmosphere (Figure 4). The initial mass loss (5%) around 120 °C could be due to residual water and/or solvent. The highest decomposition of **DMB-TT-TPA** was observed at around 405 °C and 14% of **DMB-TT-TPA** remained without ash up to 750 °C, indicating that **DMB-TT-TPA** had an excellent thermal stability. The high thermal property is profitable to the preparation of stable and durable OLED fabrication.

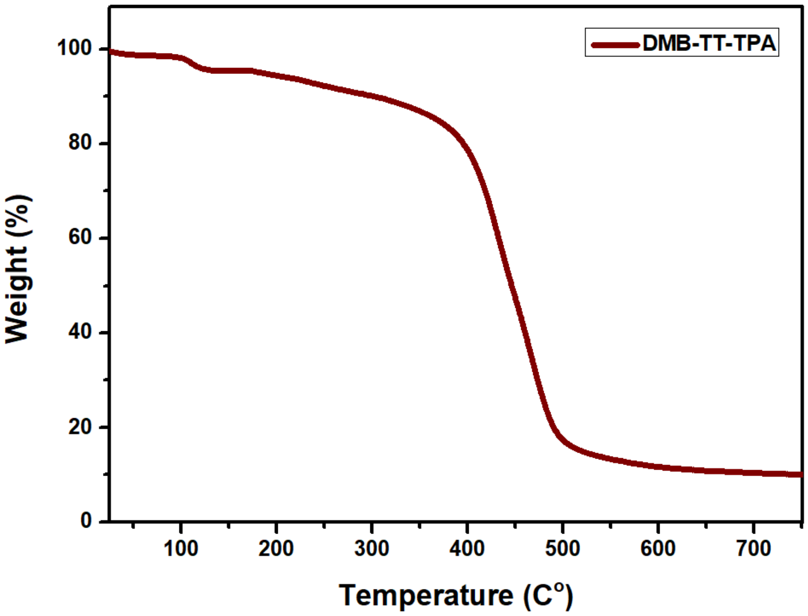

Figure 4: Thermal gravimetric analyses (TGA) of **DMB-TT-TPA**.

Computational Chemistry

Ground-state geometry optimization of **DMB-TT-TPA** was performed using density functional theory (DFT) at B3LYP/6-31G (d, p) level, Gaussian'16 software (Figure S2) [42]. The highest occupied molecular orbital (HOMO) and the lowest unoccupied molecular orbital (LUMO) energy levels were calculated to be -4.93 and -1.83 eV, respectively (Figure 5). While the HOMO electrons were distributed mainly on the triphenylamine and TT units, the LUMO was found to be delocalized through the dimesitylboron and TT ring.

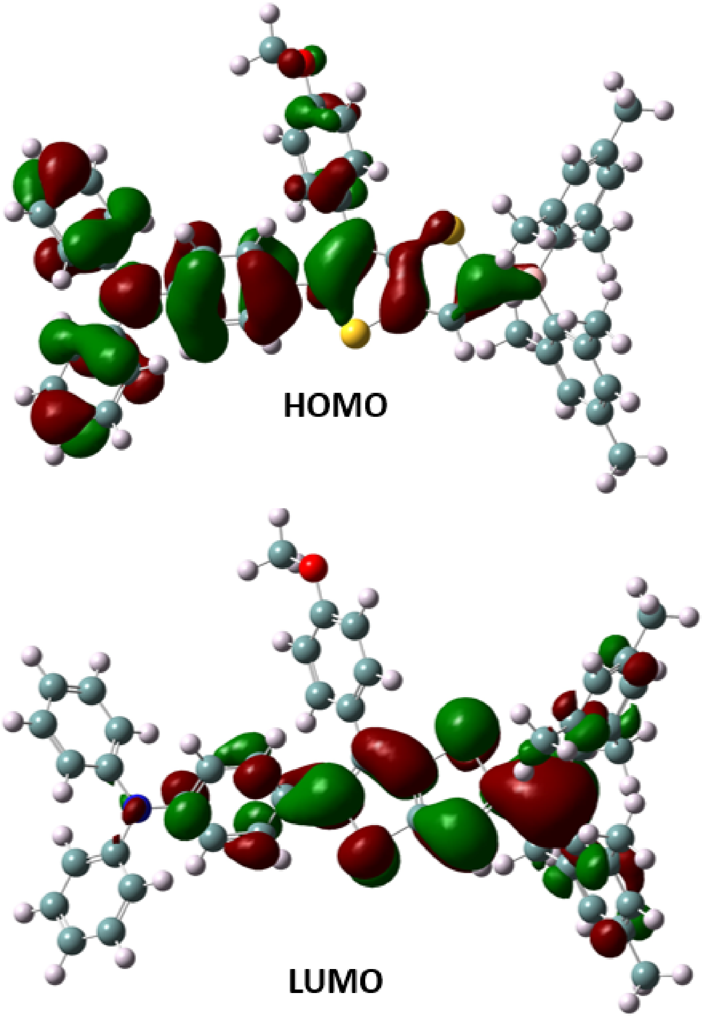

Figure 5. HOMO and LUMO diagrams calculated at the B3LYP/6-31G (d, p) level of theory.

On the basis of the optimized ground-state geometry, time-dependent DFT (TD-DFT) calculations were conducted in THF to investigate the absorption properties and theoretical band gap (Table 3). The optical band gap value (E_{optic}) was calculated to be 2.06 eV, considering the λ_{onset} (605 nm) of the UV-Vis curve. The calculated absorption maximum was centered at 470 nm (Figure S3), which was found to be in a good agreement with the experimentally determined UV-Vis spectrum.

Table 3. The HOMO and LUMO energy levels, and absorption values calculated by TD-B3LYP/6-31G (d, p) level of theory.

Compound	HOMO (eV)	LUMO (eV)	λ_{max} (nm)	λ_{onset} (nm)	E_{optic} (eV)
DMB-TT-TPA	-4.93	-1.83	470	605	2.06

Conclusion

A small fluorophore molecule, **DMB-TT-TPA**, containing dimesitylboron as an acceptor, triphenylamine as a donor linked through thieno[3,2-b]thiophen, having a 4-MeOPh group, was designed as a D-p-A modal and synthesized in 85% yield. Its photophysical properties were investigated by UV-Vis and fluorescence spectroscopies. The obtained experimental results were found to be in good agreement with computational investigations. Its OLED, where **DMB-TT-TPA** was employed as an emitter, showed a maximum luminescence efficiency of 752 cd/m^2, a maximum external quantum efficiency of 4.61%, a maximum power efficiency of 6.70% and a maximum current efficiency of 10.6 cd/A on 2.9 V turn on voltage with CIE coordinates of 0.16 and 0.51 at l_{EL}=512 nm. The OLED, optical and thermal properties indicated that composition of thienothiophene, triphenylamine and boron is highly suitable combination for fluorescent organic electronics in display technology.

Supporting Information

Supporting Information File 1

General experimental device methods and theoretical computation data.

Acknowledgements

The authors thank Dilara Gunturkun for DFT calculations, Istanbul Technical University (ITU) and Unsped Global Lojistik, Turkey, for financial support. We also thank Higher Education Council of Turkey (YOK) and TUBITAK grants to Recep Isci (PhD, 100/2000 YOK and 2211A BIDEP/TUBITAK) for financial support.

References

1. Tavasli, A.; Gurunlu, B.; Gunturkun, D.; Isci, R.; Faraji, S. *Electronics,* **2022**, *11*(3), 316.
2. Chen, Z.; Huang, Y.; Gao, J.; Zhang, L.; Ma, Z.; Liu, M.; Emrick, T.; Liu, Y. *ACS Energy Lett.* **2022,** *7* (11), 4052-4060.
3. M'Baye, G.; Klymchenko, A. S.; Yushchenko, D. A.; Shvadchak, V. V.; Ozturk, T.; Mély, Y.; Duportail, G. *Photochem. Photobiol. Sci.* **2007**, *6* (1), 71-76.
4. Takimiya, K.; Osaka, I.; Nakano, M. *Chem. Mater.* **2014**, *26*, 1, 587-593.
5. Monkman, A. *ACS Appl Mater Interfaces* **2022**, *14,* 18, 20463-20467.
6. Yu, L.; Portale, G.; Stingelin, N. *J. Mater. Chem. C*, **2021**, *9,* 10547-10556.
7. Liu, X., Lin, R., Chen, H., Zhang, S., Qian, Z., Zhou, G., Chen, X.; Zhou, X.; Zheng, L.; Liu, R.; Tian, P. *ACS Photonics* **2019,** *6,* 12, 3186-3195.
8. Oyama, Y.; Mamada, M.; Shukla, A.; Moore, E. G.; Lo, S.-C.; Namdas, E. B.; Adachi, C. *ACS Materials Lett.* **2020,** *2,* 161−167.
9. Isci, R.; Varzeghani, A. R.; Kaya, K.; Sütay, B.; Tekin, E.; Ozturk, T. *ACS Sustain. Chem. Eng.* **2022**, *10* (4), 1605-1615.
10. Jiang, H.; Peng Tao, P.; Wong, W.-Y. *ACS Materials Lett.* **2023,** *5,* 3, 822-845.

11. Tsai, M.-H.; Ke, T.-H.; Lin, H.-W.; Wu, C.-C.; Chiu, S.-F.; Fang, F.-C.; Liao, Y.-L.; Wong, K.-T.; Chen, Y.-H.; Wu, C.-I. *ACS Appl. Mater. Interfaces* **2009,** *1,* 3, 567-574.
12. Wang, J.; Liu, K.; Ma, L.; Zhan, X. *Chem. Rev.* **2016,** 116, 23, 14675–14725.
13. Schipper, D. J.; Keith Fagnou, K. *Chem. Mater.* **2011,** *23,* 6, 1594-1600.
14. Cinar, M. E.; Ozturk, T.; Thienothiophenes, Dithienothiophenes, and Thienoacenes: Syntheses, Oligomers, Polymers, and Properties. *Chem. Rev.* **2015,** *115,* 3036-3140.
15. Isci, R.; Unal, M.; Kucukcakir, G.; Gurbuz, N. A.; Gorkem, S. F.; Ozturk, T. *J. Phys. Chem. B.* **2021,** *125* (48), 13309-13319.
16. Isci, R.; Gunturkun, D.; Yalin, A. S.; Ozturk, T. *J. Polym. Sci.* **2021**, *59* (1), 117-123.
17. Gunturkun, D.; Isci, R.; Sütay, B.; Majewski, L. A.; Faraji, S.; Ozturk, T. *Eur. Polym. J.* **2022,** *170,* 111167.
18. Ozturk, T.; Rice, C. R.; Wallis, J. D. *J. Mater. Chem.,* **1995,** *5,* 1553-1556.
19. Schneider, J. A.; Dadvand, A.; Wen, W.; Perepichka, D. F. *Macromolecules* **2013,** *46,* 23, 9231-9239.
20. Isci, R.; Tekin, E.; Kaya, K.; Mucur P. S.; Gorkem, S. F.; Ozturk, T. *J. Mater. Chem. C.* **2020,** *8,* 7908-7915.
21. Isci, R.; Tekin, E.; Mucur, S. P.; Ozturk, T. *ChemistrySelect,* **2020,** *5* (42), 13091-13098.
22. Isci, R.; Wan, L.; Topal, S.; Gunturkun, D.; Campbell, A. J.; Ozturk, T. *J. Mater. Chem. C* **2022**, *10* (29), 10719-10727.
23. Turkoglu, G.; Cinar, M. E.; Buyruk, A.; Tekin, E.; Mucur, S. P.; Kaya K.; Ozturk, T. *J. Mater. Chem. C* **2016,** *4* (25), 6045-6053.

24. Isci, R.; Unal, M.; Yesil, T.; Ekici, A.; Sütay, B.; Zafer, C.; Ozturk, T. *Front. Mater.* **2023,** *10,* 1125462.
25. Chi, W.-J.; Zheng, D.-Y.; Chen, X.-F.; Li, Z.-S. *J. Mater. Chem. C* **2017,** 5 (38), 10055-10060.
26. Ozturk, S. E.; Isci, R.; Faraji, S.; Sütay, B.; Majewski, L. A.; Ozturk, T. *Eur. Polym. J.* **2023**, *191,* 112028.
27. Amna, B.; Isci, R.; Siddiqi, H. M.; Majewski, L. A.; Faraji, S.; Ozturk, T. *J. Mater. Chem. C* **2022**, *10* (21): 8254-8265.
28. Zhong, H.; Li, C.-Z.; Carpenter, J.; Ade, H.; Jen, A. K.-Y. *J. Am. Chem. Soc*. **2015,** *137,* 24, 7616-7619.
29. Isci, R.; Balkan, T.; Tafazoli, S.; Sütay, B.; Eroglu, M. S.; Ozturk, T. *ACS Appl. Energy Mater.* **2022,** *5* (11), 13284-13292.
30. Topal, S.; Isci, R.; Sezer, E.; Ozturk, T.; Ustamehmetoglu, B. *Electrochim. Acta.* **2021,** *389,* 138688.
31. Isci, R.; Baysak, E.; Kesan, G.; Minofar, B.; Eroglu, M. S.; Duygulu, O.; Gorkem, S. F.; Ozturk, T. *Nanoscale* **2022,** *14,* 16602-16610.
32. Celiker, T.; Isci, R.; Kaya, K.; Ozturk, T.; Yagci, Y. *J. Polym. Sci.* **2020,** *58* (17), 2327-2334.
33. Kutahya, C.; Allushi, A.; Isci, R.; Kreutzer, J.; Ozturk, T.; Yilmaz, G.; Yagci, Y. *Macromolecules* **2017,** *50* (17), 6903-6910.
34. Beyazit, S.; Aydogan, B.; Osken, I., Ozturk, T.; Yagci, Y. *Polym. Chem.* **2011,** *2,* 1185-1189.
35. Farokhi, A.; Shahroosvand, H.; Monache, G. D.; Pilkington, M.; Nazeeruddin, M. K. *Chem. Soc. Rev.* **2022,** *51,* 5974-6064.
36. Turkoglu, G.; Cinar M. E.; Ozturk T. *Eur. J. Org. Chem.* **2017,** *31*, 4552-4561.

37. Zhou, G.; Baumgarten, M.; Müllen, K. *J. Am. Chem. Soc.* **2008,** *130,* 37, 12477–12484.

38. Sonar, P.; Soh, M. S.; Cheng, Y. H.; Henssler, J. T.; Sellinger, A. *Org. Lett.* **2010,** *12,* 15, 3292–3295.

39. Lee, H.; Karthik, D.; Lampande, R.; Ryu, J. H.; Kwon, J. H. *Front. Chem.* **2020,** *8,* 373.

40. Xu, T.; Liang, X.; Xie, G. *Front. Chem.* **2021,** *9,* 691172.

41. Fu, Q.; Chen, J.; Shi, C.; Ma, D. *ACS Appl. Mater. Interfaces* **2012,** *4,* 12, 6579–6586.

42. Frisch, M. J.; Trucks, G. W.; Schlegel, H. B.; Scuseria, G. E.; Robb, M. A.; Cheeseman, J. R.; Scalmani, G.; Barone, V.; Mennucci, B.; Petersson, G. A.; Nakatsuji, H.; Caricato, M.; Li, X.; Hratchian, H. P.; Izmay lov, A. F.; Bloino, J.; Zheng, G.; Sonnenberg, J. L.; Hada, M.; Ehara, M.; Toyota, K.; Fukuda, R.; Hasegawa, J.; Ishida, M.; Nakajima, T.; Honda, Y.; Kitao, O.; Nakai, H.; Vreven, T.; Montgomery, J. A.; Jr.; Peralta, J. E.; Ogliaro, F.; Bearpark, M.; Heyd, J. J.; Brothers, E.; Kudin, K. N.; Staroverov, V. N.; Kobayashi, R.; Normand, J.; Raghavachari, K.; Rendell, A.; Burant, J. C.; Iyengar, S. S.; Tomasi, J.; Cossi, M.; Rega, N.; Millam, J. M.; Klene, M.; Knox, J. E.; Cross, J. B.; Bakken, V.; Adamo, C.; Jaramillo, J.; Gomperts, R.; Stratmann, R. E.; Yazyev, O.; Austin, A. J.; Cammi, R.; Pomelli, C.; Ochterski, J. W.; Martin, R. L.; Morokuma, K.; Zakrzewski, V. G.; Voth, G. A.; Salvador, P.; Dannenberg, J. J.; Dapprich, S.; Daniels, A. D.; Farkas, O.; Foresman, J. B.; Ortiz, J. V.; Cioslowski, J.; Fox, D. J. Wallingford CT, *Gaussian 09,* **2016.**